Structural Health Monitoring of Historic Ships in Dry Docks: The First Step Towards Preventive Conservation Approach

Raffaele De Risi[1,*], Marianna Ercolino[2], Nicola Grahamslaw[3], Maria Bastidas-Spence[4], Branislav Titurus[1]

[1.] School of Civil, Aerospace and Design Engineering, University of Bristol

[2.] Department of Civil and Environmental Engineering, Brunel University

[3.] SS Great Britain Trust.

[4.] National Museum of the Royal Navy.

Submitted to: *International Journal of Architectural Heritage*

* Corresponding Author: raffaele.derisi@bristol.ac.uk

Abstract

Historic ships are vital components of maritime cultural heritage, reflecting the evolution of naval engineering and design. Often preserved in dry docks, these vessels face structural challenges due to their prolonged grounding, which they were not originally designed to endure. Effective conservation strategies require robust support systems that prevent stress concentrations and mitigate the risks of environmental and vibrational factors. The long-term preservation of historic ships also demands an integrated understanding of the ship's structural health, the dock's condition, and the adequacy of the support system. To address these complex preservation needs, this study presents a feasibility study on employing vibration-based SHM for two iconic British vessels: the SS Great Britain in Bristol and the Cutty Sark in London. This paper bridges a significant gap in the literature by demonstrating the potential of SHM for historic ships in dry docks, underscoring the necessity of a multidisciplinary approach that integrates structural, environmental, and geotechnical considerations to ensure the sustainable preservation of maritime heritage.

Keywords: *Non-destructive testing, Operational Modal Analysis, Single Value Decomposition, Cultural Heritage, MonStr Sensors*

1. Introduction

Historic ships are vessels typically constructed over a century ago that played significant functions in public transport, trade, and warfare. These ships are rarely intact as they had to survive combats, severe weather conditions, and general age deterioration. In the UK, great examples of well-preserved vessels are the H.M.S. Victory in Portsmouth (Aberg, 2005), the Cutty Sark in London (Douglas, 2012), the HMS M.33 in Portsmouth (Schleihauf, 2000), the SS Nomadic in Belfast (Davis, 2024), and the SS Great Britain in Bristol (Watkinson et al., 2005). Moreover, more historic ships are foreseen to be located in dry dock such as the HMS Unicorn (https://www.hmsunicorn.org.uk/) in Dundee. Historic ships have an essential role in national maritime cultural heritage because they demonstrate the evolution of maritime engineering practices. These ships are often permanently placed in dry-dock to protect their historical value (Waite, 1997). Dry docking offers different advantages: (i) easier access to the asset and display of the underwater body, (ii) lower maintenance costs with respect to floating ships, and (iii) improved capabilities of controlling the ageing components and preventing degenerative phenomena (e.g. corrosion) maximising the longevity of the original ship's character. However, these ships were designed to stay afloat and not sit on the ground for long periods. So, the main risk when dry-docked is that the ship could collapse under its own weight. Moreover, they are exposed to new risks, such as external environmental actions (e.g., traffic vibrations and extreme events due to climate change). A more extensive description encompassing also social aspects of dry docking is provided in Millar et al. (2024).

When docked, ships require a robust support system that should be "sympathetic" to the unique ship's nature and age. This system must redistribute the ship's weight by avoiding stress concentrations on the fragile hull (House 2015). The support structure should remain healthy over time under the excitations induced by visitors, ground-borne vibrations, and environmental loadings such as temperature, humidity, and wind. Also, long-term effects such as possible settlements, material creep, and corrosion should be accounted for. To better understand the main criticalities associated with historic ships in dry docks, it is necessary to have an overview of the main features of dry docks and the key structural elements that permanently support such ships.

Dry-docking has its roots in ancient civilisations (Rehler and Bottger, 1964), where ships were pulled ashore for repairs. The first recorded dry docks were built in the 16th century in the Netherlands, United Kingdom and China. The demand for dry docks increased as the maritime industry grew in the 19th century (Otter, 2003). The critical components of a dry dock include (a) the entrance gate, which is a movable barrier that seals the dock; (b) the dock floor, i.e. the flat (or slightly sloping), solid surface where the ship rests; (c) the dock walls or sidewalls, serving essential functions such as structural support, holding back the surrounding water and/or soil, and providing attachment points to secure the ship during the docking process to prevent it from shifting. Sidewalls are usually made of a series of horizontal steps (also known as altars) running around the contour of the dock, broken up by a series of flat inclined slides. Most dry docks have floor and sidewalls made of stone masonry. Sometimes, the floor has encased timber elements (installed in vertical recesses) historically used as sliders. From a structural and geotechnical point of view, the dock structures may be affected by water seepage, material degradation, and settlements. All these phenomena can be a severe problem for the structural system supporting the ship and, in turn, for the ship itself.

Figure 1 shows the most common approaches used for docking historic ships in dry docks. In many cases, if the keel beam is strong enough, the ship is supported by timber blocks located at the centre-bottom of the ship (Figures 1A-1C). These blocks, typically made of timber and of different heights to accommodate the keel profile, are distributed in specific positions along the keel beam, creating a discontinuous line of supports. In almost all cases, a single support line at the centre cannot guarantee stability. For the part of the ship's hull where the cross-section is sub-rectangular, the bottom part of the hull is flat, and the bilge keels are strong enough, additional lateral support systems, known as bilge blocks or side blocks, made of timber (or a combination of timber and steel brackets) are used to stabilise the ship in the dry dock (Figure 1A). If the side blocks cannot be used, sub-horizontal struts (also known as shore struts, breast shores, or simply shores) stabilise the ship (Figure 1B). An alternative to side shores is the adoption of sub-vertical struts, also known as dock struts (Figure 1C). When struts are used, sacrificial timber elements are typically placed between the struts and the ship's hull. The elements are known as wedging timber elements or soft caps. Moreover, when struts are used, these are located in positions corresponding to the rigid ribs of the ship, i.e. where steel frames are available in correspondence with the main decks' beams. This simplifies the load transfer between the ship structure and the supporting structure in the dry dock. An example of Figure 1A support system is the SS Nomadic in Belfast (Davis, 2024). Examples of combinations of support systems presented in Figures 1A-C are the H.M.S. Victory in Portsmouth, UK (Aberg, 2005) and the SS Great Britain in Bristol, UK (Watkinson et al., 2005).

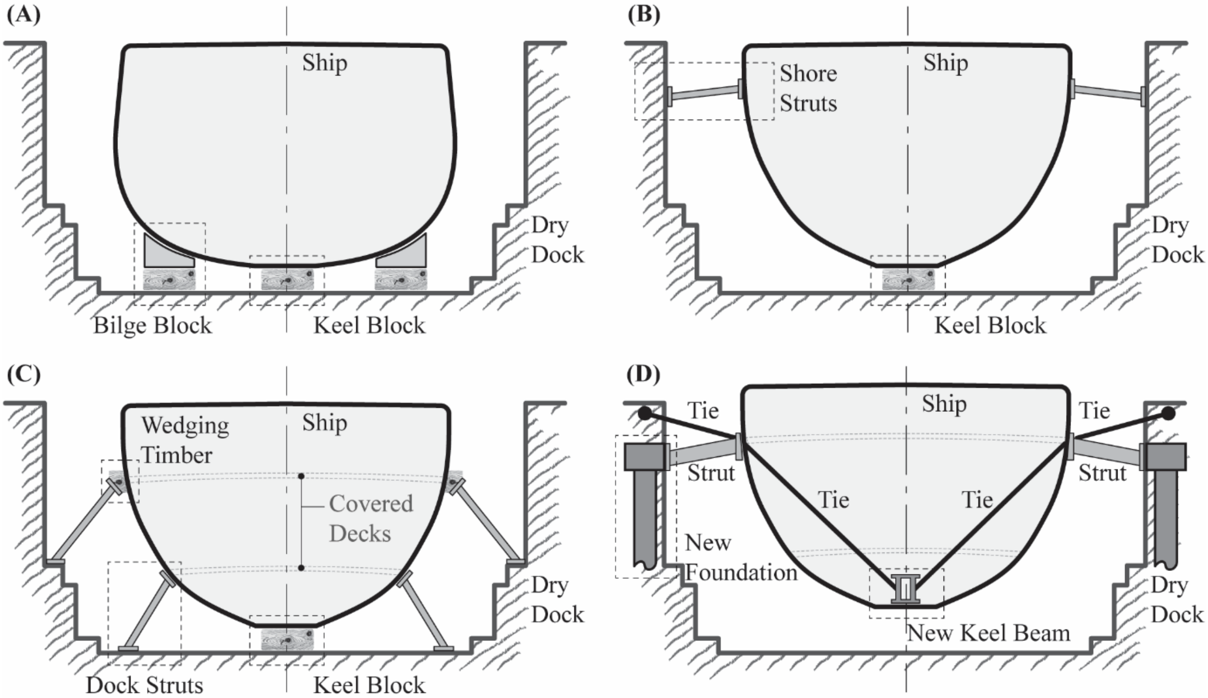

Figure 1 – Different support system configurations in dry docks for historic ships. (A) Support on keel and bilge blocks. (B) Support on blocks and stabilising sub-horizontal shore struts. (C) Support on blocks and stabilising sub-vertical dock struts. (D) Suspended support configuration.

Finally, if the hull and the keel beam are not in good condition, an option is to suspend the ship to reinforced dock walls by creating a strut-and-tie support system and a new keel beam supporting the main internal stanchions of the ship (Figure 1D). Such a solution requires both geotechnical and structural works (e.g. piles and cap beams) on the docksides and extensive steel structural works inside the ship. An example of such a support system is that of the Cutty Sark in London (Douglas, 2012).

From a conservation point of view, three main macro-components can affect the long-term health status of a historic ship in a dry dock: (1) the status of the ship's structural system, including the hull, the keel beam, and the stiffener ribs; (2) the status of the structural support system, including the timber supports, the struts, the timber interface elements between the struts and the hull, and the geotechnical conditions; (3) the dock status, including the state of the stone masonry on the dock's floor and altars. Therefore, the conservation problem for such pieces of cultural heritage is very complex, and it requires a holistic multidisciplinary approach to assess, interpret, conserve, document and strategically manage such important assets.

In this context, vibration-based Structural Health Monitoring (SHM) has been proven an excellent tool for supporting the preventive conservation of cultural heritage, averting future damage and prolonging the life of cultural heritage assets (Ceravolo et al., 2016; Clementi et al., 2021). SHM was used for religious buildings (Alaggio et al., 2021; Cigada et al., 2017; Formisano et al., 2021; Pecorelli et al., 2020), obelisks (Bongiovanni et al., 2021), and towers (Azzara et al., 2021; Barsocchi et al., 2021; Fiorentino et al., 2019; Milani et al., 2021; Standoli et al., 2021). Although SHM is recognised as a consolidated tool for naval inspections (Lin and Dong, 2023), the literature does not provide examples of historic ships in dry docks. To fill such a gap, this paper offers a feasibility study to determine the possibility of using vibration-based SHM as a non-intrusive diagnostic tool by looking at natural frequencies, modal damping values and vibration mode shapes of historic ships in dry docks.

This research paper consists of five main sections. **Section 2** explains the methodological approach, comprising an idealised dynamic model of a docked ship, the rational sensor placement, and a discussion of signal processing. **Section 3** describes the investigated case studies: the SS Great Britain in Bristol and the Cutty Sark in London. **Section 4** presents the monitoring results of the two case studies and discusses similarities and differences. Finally, **Section 5** wraps up the main conclusions and identifies limitations, and future research needs on the topic.

2. Methodology

2.1 Simplified Model and Sensors Placement Strategy

When designing a vibration-based SHM system, creating a virtual model of the asset to be monitored is often beneficial, as it provides a preliminary understanding of the expected vibration modes and frequencies (Pregnolato et al., 2022). These models are usually finite element models (FEM) that allow identifying the most strategic (or optimal) locations for sensors (Abu Shehab et al., 2024) by using consolidated procedures such as the Effective Independence method (EFI, Kammer, 1991) or the AutoMAC (Civera et al., 2021). Unfortunately, creating finite element models of complicated systems, such as historic ships in dry docks, is not always possible. This can be time-consuming and always associated with a significant degree of uncertainty. In some cases, the blueprints of the support structure are not available, and it may not be straightforward to cope with a new survey, which may not be able to provide all the needed data (e.g., geometry and material properties of the supports). To overcome such an issue, for this study, we adopt the simplified strategy, which combines an understanding of the anticipated rigid body activity and assumed flexural motions (Hageman and Drummen, 2019) with other limitations typically imposed by the measurement system, such as (i) the number of channels, (ii) the sensor placement constraints (e.g. accessibility or orientation). Depending on the specifics of the ship's support system and initially ignoring the dynamic flexibility of the ship, the fundamental contributions to the overall rigid body motion could consist of a combination of three rotations and three translations. For instance, as exemplified in conceptual Figure 2, the rotational movements that a ship can have as a rigid body are (1) the roll, i.e. rotation along the longitudinal horizontal axis of the ship (Figure 2A); (2) the pitch, which is the rotation around the transverse horizontal axis of the ship (Figure 2B); and (3) the yaw, which is the rotation around the vertical axis (Figure 2C).

Moreover, when adopting this approach, the support structure can typically be idealised with springs. Specifically, the cross-section can be associated with vertical, horizontal, and rotational springs, where the rotational spring is created by the lever arm between the supports (e.g., Figure 1C). The pitch and the yaw can be associated with Winkler-like spring beds, reflecting the discontinuous nature of the supports.

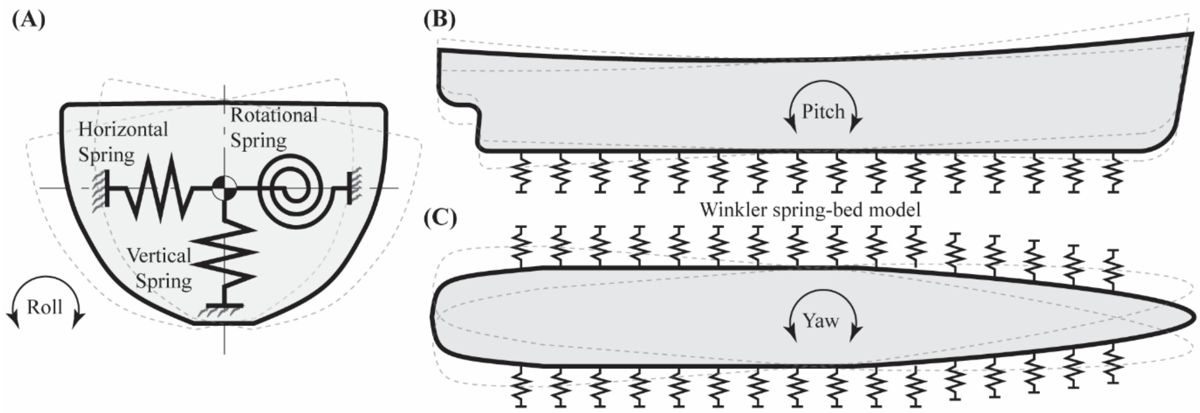

Figure 2 – Simplified dynamic model of a docked ship illustrating (A) roll (transverse cross-section view), (B) pitch (longitudinal cross-section view), and (C) yaw motions (top planar view).

Therefore, this simplified dynamic representation clearly shows that the appropriate locations for the sensors can be the edges of the decks towards the bow and the stern, where the maximum dynamic responses are expected. In this spirit, in the case of suspended support configuration (Figure 1D), ideally, sensors should also be placed on the keel beam. However, some practical aspects may prevent the installation of sensors in the desired places. First, ships may have inaccessible areas; second, bulkheads among different compartments can complicate the installation of cables and interrupt the signal of wireless sensors. Therefore, the optimised sensor placement should also account for accessibility and other practical aspects of installation.

Another practical aspect that should be considered is the mounting system. Mounting options include direct stud mounting, wax mounting, magnetic mounting, and various other methods in between (Dumont et al., 2016). Whatever the method, it must be sympathetic to the ship's historical nature, not damage the part or material on which the sensors are installed and must be tested for reliability before the final installation. A final aspect that should be considered for optimising the sensor placement is the number of available channels and the capability of the adopted sensors. Ideally, sensors capable of recording accelerations along three directions should be used. However, due to budget constraints or the limited number of available channels of the data acquisition system, a selection should be made on which direction and where to measure to maximise the level of acquired information. Usually, such optimisation is conducted by looking at simple kinematic rules, such as considering the system's sectional shape to be rigid (Gonzalez-Fernandez et al., 2023).

2.2 Signal Processing and Operational Modal Analysis

The data from the sensors can be acquired continuously over several months (long-term) or during specific periods of the year (short-term) to study the effect of seasonality on the response of the maritime heritage of interest. Ideally, a continuous acquisition system should be preferred in combination with automatic identification of the system's dynamic features (Pecorelli et al., 2020). When examining long-term data, potential shifts in frequencies or vibration modes unrelated to seasonality can indicate damage to some system components. Such variations constitute an alarm that should trigger a deeper inspection to find the cause of damage. For example, high-order spectral analysis (HOSA, Nikias and Mendel, 1993) can be used for damage detection.

Before moving to more advanced damage detection techniques, this work's scope is to investigate the suitability of vibration-based SHM for historic ships in dry docks as a source of data and diagnostic parameters that can inform preventive conservation. Therefore, evaluating contemporary tools and methods when identifying the modal characteristics of potential diagnostic significance under normal operational conditions is instrumental.

Regarding the signal processing, the acquired data need to be treated appropriately to infer helpful information. Inadequate signal processing, a low sampling rate, and inappropriate filtering with inaccurate cutoff frequencies may distort processed signals in shape, phase, and amplitude (Karanikoloudis et al., 2021). In this study, a simple zero-phase digital filter with transfer function coefficients of a 4^{th}-order bandpass digital Butterworth filter (Mitra, 2001) for the frequency range between 0.2 Hz and 50 Hz has been used for preliminary signal processing. This frequency interval is suggested to remove any unlikely long-period large-displacement motion and to avoid catching any high-frequency local mode inconsistent with the idealised motion presented in Figure 2.

Once the signals have been adequately treated, the Operational Modal Analysis (OMA) (Rainieri and Fabbrocino, 2014) can be conducted. OMA is a technique used to determine a structure's dynamic characteristics (such as natural frequencies, mode shapes, and damping ratios) under actual operating conditions without requiring controlled or artificial excitation (Rosso et al., 2023). In other words, under certain assumptions, OMA measures the structure's response to ambient vibrations or operational forces, such as wind, traffic, or any other ground-borne vibrations. Considering the current status of this technique, four main activities are herein proposed and performed for the preliminary OMA of docked ships: (1) overlay of the measured signals' power spectral density (PSD) graphs (Akan and Chaparro, 2024) for all the sensors distinguishing the different directions; (2) initially evaluate the time-varying frequency content of the acquired signals using the spectrograms (Oppenheim and Schafer,1999) and to check for the signal's non-stationarity; this exercise is not to check the presence of damage but to confirm the observable dynamic characteristics as the representative features of the system (it is worth mentioning that a first visual screening of the signal's spectrogram can already offer information such as specific time patterns and help identify the valuable part of the signal with respect to the noise); (3) select the time interval of interest and compute the stabilisation diagram using (Peeters et al., 2004) to identify the stable frequencies and, if needed, the modal damping values; and (4) compute the vibration modes using Singular Value Decomposition (SVD, Brincker and Ventura, 2015). This four-step process will be used in the following case studies to gain a deeper understanding of the operationally observable modal characteristics of the two significant dry-docked ships.

More details are provided herein on the previous points 3 and 4. Direct analysis of the measured PSDs readily permits the determination of the dominant response frequencies excited during the data collection. However, the use of formal theory of linear dynamic system and stabilisation diagrams provides a more objective identification approach. Since the monitoring test relied only on environmental sources of excitation, assuming they can be approximated as white noise within the frequency range of interest, the stabilisation diagram can be constructed using the identified response half PSDs (Guillaume 2006). However, the operational nature of the field experiment, the potential presence of any extraneous excitations, and the limited system's observability still create a degree of ambiguity when interpreting these diagrams. In such a context, a judicious frequency down-selection combined with further prior system insights must be used to increase identification confidence.

In general, the calculation of stabilisation diagrams consists of the least square-based fitting of the experimental data with a linear time-invariant dynamic system of gradually increasing order. The aim is to determine the underlying dynamic characteristics represented by the complex-valued poles. These poles contain information about the natural frequencies and modal damping ratios of the observed dynamic system. If a certain system pole for multiple consecutive model orders remains approximately the same and the above excitation assumption is broadly satisfied, the pole is described as stable and becomes a candidate for the true physical pole. The assessment concerning the pole's stability is traditionally based on the visual assessment of the imaginary parts of the calculated poles. This work adopts a refined approach that helps determine the pole structure based on additional criteria (e.g., Jaytilake et al. 2024). Finally, where further required, the stabilisation diagrams provide a basis for various advanced system identification algorithms, such as the PoliMAX algorithm (Peeters et al., 2004). This research uses the acceleration PSDs, and the stabilisation diagrams are calculated using the existing functionality available in Matlab's Signal Processing Toolbox Version 2022a (Matlab 2023).

3. Case studies

The proposed SHM technique was assessed on two different case studies of dry-docked ships in the UK. The first case is a three-hour acceleration monitoring test of the SS Great Britain in Bristol, conducted in February 2024 over a very windy day with a mean wind velocity of about 10m/s and gusts reaching 20m/s. The second case is a twelve-hour acceleration monitoring test of the Cutty Sark in London, conducted in July 2024 during a warm, quiet night, with average wind velocities below 4m/s. Unfortunately, no high-resolution wind data is available; therefore, it is not possible to correlate wind characteristics with the dynamic behaviour of the ships. The same set of sensors and data acquisition systems were employed for both case studies. In the following, the case studies are detailed. Then, the adopted sensors and the acquisition system are described. Finally, the sensor configurations for the two case studies are presented.

3.1 SS Great Britain

The SS Great Britain (Figure 3A), designed by the renowned engineer Isambard Kingdom Brunel, is a landmark in maritime history. Launched in 1843, she was the world's first large iron-hulled, screw-propelled steamship, representing a significant leap forward in shipbuilding technology. In fact, at that time, being provided with an innovative engine in the central part, the ship was faster and more energy-efficient than smaller wooden vessels. With a length of about 98 metres (321 ft), a width of about 15.5 metres (51 ft) at the widest point, and weighing 3,674 tons, the SS Great Britain was the largest ship in the world at the time of her launch. The ship was also equipped with six masts to utilise wind as an additional source of propulsion. The ship was initially designed for transatlantic service between Bristol and New York, capable of carrying passengers and cargo at unprecedented speed. However, she ran aground in 1846 due to a navigational error. After almost a year, the SS Great Britain was converted to a passenger and cargo vessel for long-distance voyages, including routes to Australia. For nearly 30 years, the SS Great Britain transported thousands of immigrants to Australia before being converted into a cargo ship. Her working life ended in 1886, and she was scuttled in the Falkland Islands, where she lay for nearly a century. In 1970, the ship was salvaged and returned to Bristol, where she underwent extensive restoration. Today, the SS Great Britain serves as a museum ship and a symbol of Britain's industrial innovation.

From a structural point of view, the ship has a metal deck, two longitudinal bulkheads, and a series of watertight compartments running along the ship's length. The hull is made of a metal sheet supported by stiffening steel ribs. The central part of the ship hosts the engine and its support structure. This part is heavy and comparatively rigid. The ship sits in a covered dry dock (Figure 3B) in a humidity-controlled environment to reduce corrosion progression (Ardakani et al., 2023). The support system is a combination of Figure 1A and Figure 1C; the hull is supported by timber keel blocks, timber bilge blocks and sub-vertical dock steel struts having a Hollow Circular steel Section (CHS). The top part of the struts is connected to the ship with wedging timber blocks acting as a soft cap. The external diameter of the struts is 114.3mm; however, their thickness is unknown. The bottom part of the strut is connected to the dock floor, and these connections can be idealised as simple hinges. The struts are also adjustable in length to accommodate future needs in the supporting system.

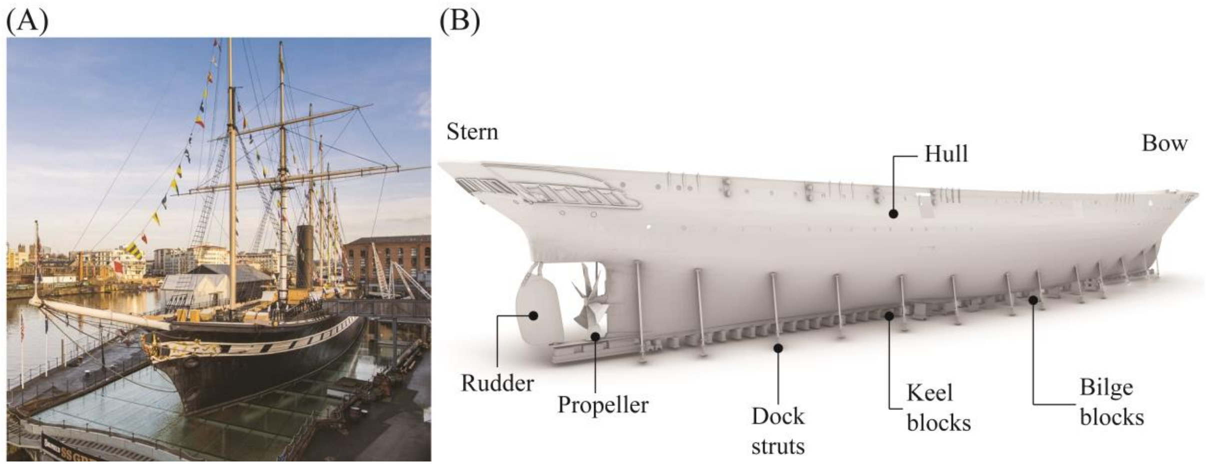

Figure 3 – (A) Aerial photo of the SS Great Britain from the bow. (B) Schematic representation of the support system in the dry dock.

From a conservation point of view, the timber blocks, the timber caps, and the health of the struts are certainly of interest. They offer critical support to the ship and can be idealised as spring elements. Therefore, the system's dynamic is heavily affected by their health status. Indeed, variations in the conditions of these components will be reflected in potentially reduced axial stiffness and, therefore, lower frequencies. However, it is essential to recognise that variation in the system dynamic may also be due to other factors such as seasonality; for example, high external temperature may lead to the expansion of the struts. Therefore, it is important to have multiple vibration monitoring readings over the seasons to avoid confusing damage with other natural factors.

3.2 Cutty Sark

Cutty Sark (Figure 4A) is the last remaining extreme clipper in the world. Launched on November 22, 1869, in Dumbarton, Scotland, it embarked on its first voyage from London to Shanghai on February 16, 1870. Now over 150 years old, the ship features two enclosed decks and one open-weather deck. Much of its original hull fabric remains intact from its initial construction. The Cutty Sark has the distinctive design features of clippers: a long, slender timber hull (84 meters long and 11 meters wide), a sharp bow that cuts through waves, and three raked masts. The original iron stanchions between the masts support the ship's iron framework. The structural elements are visible, including the wrought iron frame, wooden hull planks, and Muntz metal sheathing that covers the planks.

In 2004, an extensive conservation effort was carried out to restore this historic ship to its original splendour and ensure sustainable financial support for its preservation for future generations. By 2006, work commenced to stop the degradation of the frames and reinforce the vessel structure. The ship was transferred from its previous supports onto a new permanent steel framework to relieve pressure on the keel and maintain its distinctive form. The ship was elevated 11 feet (~3.3 meters). The 963-ton ship was carefully raised in 100 mm increments by 24 hydraulic jacks, then secured in place using 24 strut-and-tie elements (the blue elements in Figure 4B). These steel elements suspended the new keel beam. Therefore, such a support structure is similar to the one represented in Figure 1D. To prevent longitudinal movements, sixteen diagonal straps (eight for each side) are installed in the central part of the ship between the top pile cap and the steel support elements presented in Figure 4B. These diagonal straps cannot be seen in Figure 4B as they are overlaid by the other diagonal struts that fall in the same vertical plane as the main suspension struts.

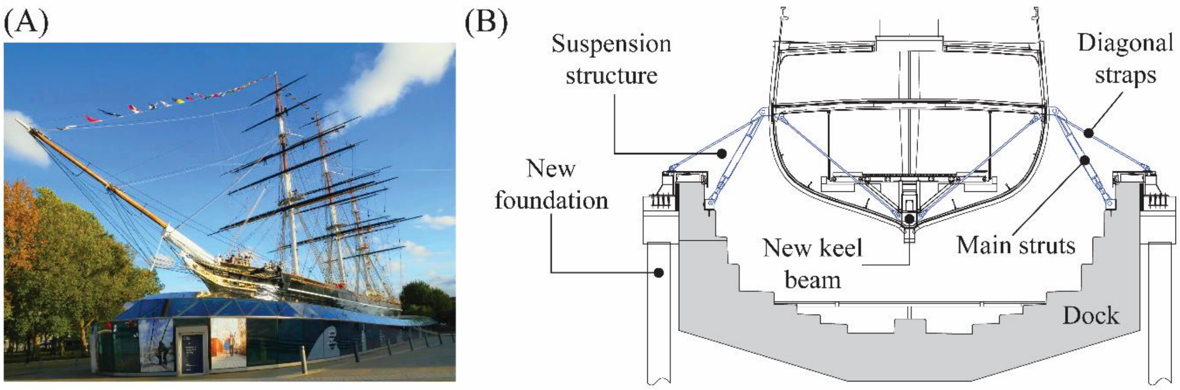

Figure 4 – (A) Frontal photo of the Cutty Sark from the bow. (B) Schematic representation of the support system in the dry dock.

From a conservation point of view, this structural support system poses similar concerns to those presented for the SS Great Britain. The difference with respect to the previous case study is that there are no timber caps or timber blocks, and the steel connection elements become critical components of systemic structural reliability. Changes in the geotechnical system, tightness of the bolts or potential fatigue problems for the welded connections may lead to larger deformability and lower frequencies.

3.3 Sensors and Data Acquisition System

The ASDEA's MonStr sensors were used (Figure 5A) to complete the test campaigns in both case studies. Each unit uses a MEMS-technology sensor with a triaxial accelerometer (Aceto et al., 2022; Boccagna et al., 2023). These sensors have a frequency range of 0÷1000 Hz, allowing for multiple acquisition frequency rates (spanning from 125Hz to 4kHz with an integrated low-pass filter for a frequency equal to a quarter of the sampling one) and multiple maximum acceleration ranges (from ±2g to ±8g). The declared spectral noise density is 25 µg/√Hz. For both case studies, the maximum acceleration was set to ±2g, and the sampling frequency was established to 500 Hz, offering the best trade-off between the risk of losing the useful or relevant dynamic behaviour and the size of the output files (discussed later). Once deployed, the sensors were connected to an ethernet PoE switch via CAT5 cables (Figure 5B); the switch was connected to a computer where the acquisition software ran. The output was saved as HDF5 files containing records for all sensors. It is possible to automatically split the files in 1-hour recording when long monitoring is carried out; such an option was adopted for the examined case study as it makes files more manageable.

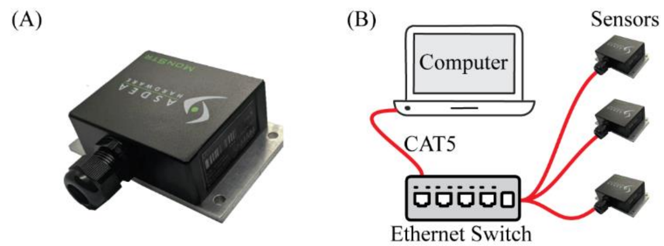

Figure 5 – (A) Photo of a MonStr sensor. (B) Schematic representation of the sensor network.

3.4 Sensors Mounting and Placement

Due to different conditions and constraints for the two case studies, two sensor mounting techniques have been used. Sensors have been installed on magnetic stands for the case of the SS Great Britain and have been fixed with hot glue on the Cutty Sark. Before the monitoring campaign, these two techniques were tested in the Earthquake Laboratory at the University of Bristol (a.k.a. EQUALS Lab), where the two mounting techniques were compared with a rigid mounting system (with steel clamps) by using the available shaking table. The signals recorded with the three sensors (i.e. the clamped one, the one mounted with hot glue, and the one mounted with magnetic stand) were identical up to a maximum acceleration of 1g (See Appendix A). Therefore, the mounting techniques have been deemed reliable for the vibration-based SHM, considering that the expected accelerations on-site are much lower than the ones imposed in the lab.

Figure 6 shows the location of the sensors for the two case studies. Their orientation is such that the x-axis and y-axis correspond to the longitudinal and transverse directions of the ship, respectively. The z-axis is the vertical one. The longitudinal axis is inclined 63° anticlockwise and 15° anticlockwise with respect to the north for the SS Great Britain and the Cutty Sark, respectively. For both case studies, the accelerometers are all located at the weather deck level, and as explained in Section 2.1, they are at the edges of the decks towards the bow and the stern. Based on their availability, five sensors were used for the SS Great Britain; seven sensors were used for the Cutty Sark. In both cases, one sensor was located close to one of the vertical elements: on the SS Great Britain, sensor A5 (Figure 6A) was located at the base of one of the masts (the third one from the ship's bow, i.e. the closest to the funnel); on the Cutty Sark, sensor B7 (Figure 6B) was located at the base of the central mast. The four A1 to A4 sensors of the SS Great Britain were located at the four edges of the engine compartment (the grey area in Figure 6A), spanning area around the central chimney. The six sensors B1 to B6 of the Cutty Sark were equally spaced on the outer edge of the deck.

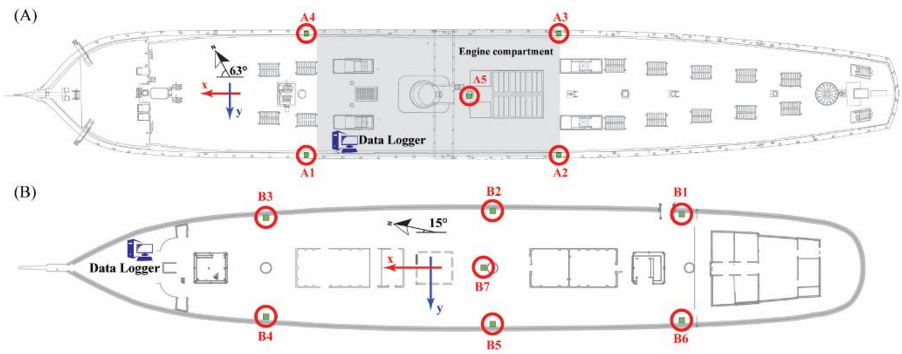

Figure 6 – Sensor and data logger placement for the (A) SS Great Britain and the (B) Cutty Sark.

In both cases, the data logger (the blue logos in Figure 6) was located in one of the covered storage areas on the deck, where power was also available. The sensors were connected to the data logger, passing through an 8-port PoE switch with CAT5 cables. Commercial CAT5 30m-long cables suitable for external applications were used. Therefore, around 180m and 270m long cables were laid down for the SS Great Britain and the Cutty Sark, respectively. Although there were no visitors during the measurements, the cables were laid down to reduce any entanglement and trip hazards to a minimum. Extensions were needed for some of the cables; extensions were created using RJB45 connectors. The exposed RJB45 connectors were protected with plastic sheets as a waterproofing strategy.

Figure 7 shows a sketch common to the two ships later used for the OMA. A simplified polygonal representation is used for the sake of simplicity. Precisely, only the central "pyramid" is plotted, and the stern and bow are neglected because of the lack of sensors in those locations.

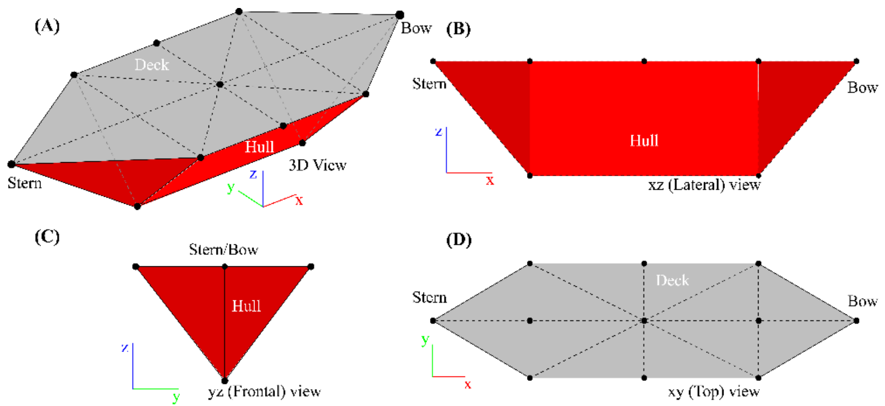

Figure 7 – Schematic representation of a generic ship layout for the OMA.

4. Results

The records of both test campaigns were split automatically into 1-hour outputs to create manageable output files. These were manually combined during post-processing into files of 3 hours for each sensor, which allows for easier data handling. The post-processing also comprised time alignment among the sensors and resampling to 2048 Hz. Finally, filtering, as explained in Section 2.2, was performed.

For both case studies, two primary sources of ambient excitation were assumed to be present. The first was wind, and the second was ground-borne vibrations. Apart from the wind, already described above, both ships are situated in areas protected with respect to primary urban traffic (a few hundred meters from main roads); however, heavy vehicles such as buses or lorries could still have induced vibrations. Unfortunately, it was not possible to install any sensor on the ground to measure ground-borne vibrations appropriately; this is because sensors would have been unsupervised and potentially exposed to unrecorded accidents.

4.1 SS Great Britain

For this case study, a 3-hour long monitoring test was conducted. Figure 8 shows the signals, in terms of accelerations, acquired by the sensor A1 during the three hours of recording for the x, y, and z directions (Figure 6A). Similar results are obtained for all other sensors. The accelerations recorded along the transverse and vertical directions are always larger than those along the longitudinal direction. This indicates that the structural support is stiffer along the longitudinal direction with respect to the other two directions. Moreover, during the test, the wind was mainly blowing along a direction of 45 degrees with respect to the north, which is almost orthogonal to the longitudinal direction of the ship. Also, the accelerations recorded along the transverse directions are slightly larger than those recorded along the vertical direction. Furthermore, the spectrograms of the three signals (Figure 8) indicate that the data contain interesting features that can be further studied. Given the apparent stationary nature of these features, it is assumed that the system and its environment did not undergo significant changes within the observation period.

A different way of presenting information from all the installed sensors is to plot the Power Spectral Density (PSD) for all sensors for the three directions, x, y, and z, separately. Figure 9 shows the PSD plots for all the sensors for both accelerations and displacements (obtained by dividing the acceleration amplitude by the square of the circular frequency). Results show that the PSD plots substantially overlay and that clear peaks can be identified for all three sensing directions. Moreover, as expected in the case of globally active low-frequency modal patterns, some peaks are common for more than one direction. This aspect indicates that possible spatially-rich vibration modes exist, as expected from Figure 2. A noticeable difference can be observed only for the z-direction for the sensor A5. This is due to the local behaviour of the mast close to the sensor. Moreover, it is interesting to note that for the y direction, the PSD plots of the pairs of sensors on the same side of the ship (i.e. A1-A2 and A3-A4, Figure 6) tend to match better than the pairs on the same transverse cross-section of the ship (i.e. A1-A4 and A2-A3, Figure 6). This indicates that the acceleration levels at the two sides of the ship are slightly different in amplitude. This difference is more visible for higher frequencies (i.e. larger than 10 Hz). Such a difference is observed because the support structure may not behave perfectly symmetrically due to geometrical or material factors. Moreover, a large crack existed in the starboard side of SSGB which was repaired with a different material (steel rather than wrought iron). It is noted that particularly distinct and rich y-z (transverse-vertical) sectional vibration activity is concentrated in the frequency range between 2 Hz and 5 Hz.

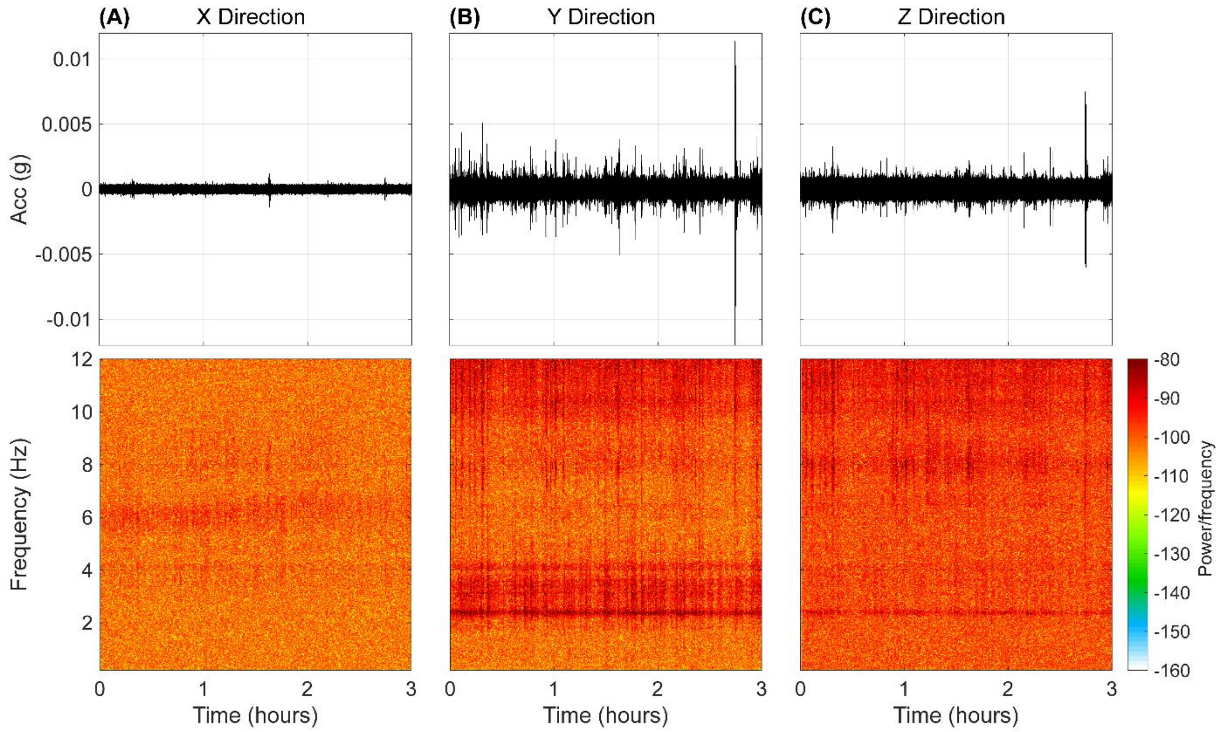

Figure 8 – Acceleration and spectrogram for the sensor A1 and for the (A) x, (B) y, and (C) z directions.

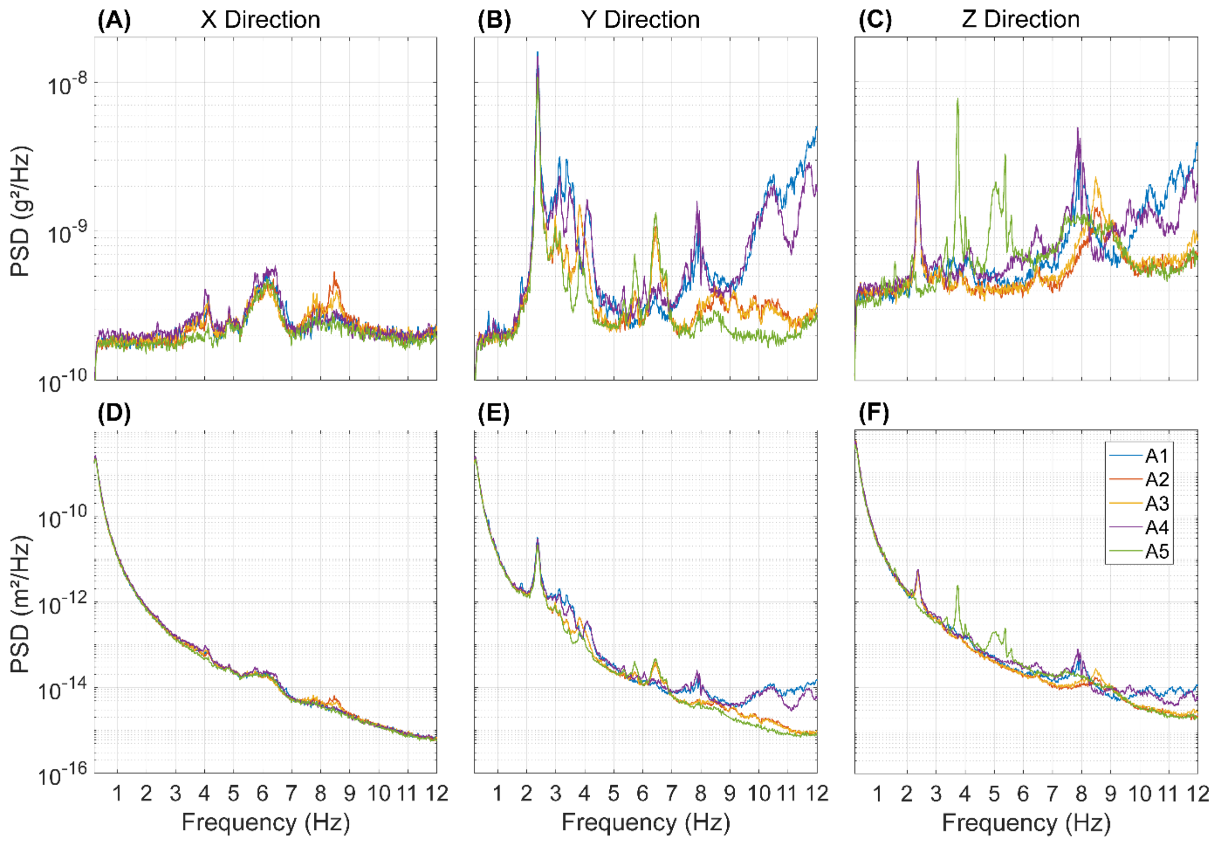

Figure 9 – Welch's Power Spectral Density plots for all sensors and for the (A,D) x, (B,E) y, and (C,F) z directions in terms of accelerations (A-C) and displacements (D-F).

Figure 10 shows the results in terms of stabilisation diagram; the following features are included in such a diagram: (1) the aggregate PSD of the accelerations in solid red line for each particular direction; (2) the numerically estimated system poles represented by their imaginary parts (the candidate natural frequencies) denoted by the blue cross markers; (3) the cumulative statistical indicator to facilitate selection of the dominant stable frequencies denoted by the grey dashed lines; (4) the selected dominant frequencies associated to particular resonance peaks. The indicator is calculated as the non-parametric probability distribution function of the identified frequencies. The candidate dominant frequencies can be determined using the peak values of the indicator function. The adopted algorithm can autonomously identify the key features of interest (frequencies) as those that are above a certain percentile (95th percentile in this case, deemed suitable according to typical one-side confidence intervals) of the recognised peaks. If the dominant features are deemed to belong to the system poles, their real values correspond to the modal damping. These values (ranging between 0.7% and 2.6%) are reported along with the frequencies for each identified dominant vibration feature.

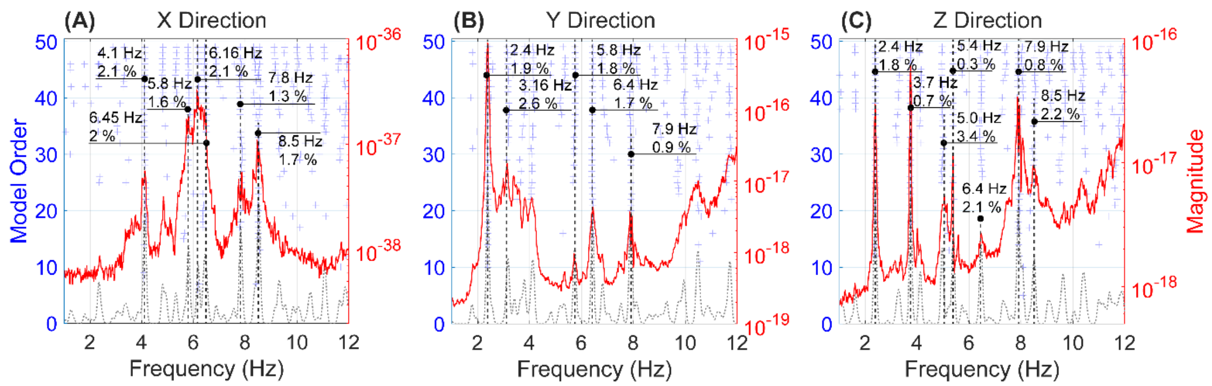

Figure 10 – Stabilisation diagram for all sensors and for the (A) x, (B) y, and (C) z directions.

From the stabilisation diagram, a frequency content emerges that could be either characteristic of the structural system or external sources such as wind excitation. Unfortunately, no information on wind gusts is available for the monitoring day. However, in the range of investigated frequencies (i.e. 1 to 10 Hz), according to the Davenport spectrum, the gust contribution should have been negligible (Davenport 1961). In the present context, wind gusts are likely to serve as a useful source of intermittent transients rich in the low-frequency modal content. In this way, they are perceived as an important factor enriching the collected operational acceleration responses. Further, wind could generate distinct periodic forcing for steady wind flows due to vortex shedding around the bluff bodies in an airstream, such as the masts (Vickery and Basu, 1983). Assuming a Strouhal number of 0.2 (typically taken for cylindrical structures), a range of frequencies between 1 and 10 Hz, and a range of diameters between 40 cm and 80 cm, the wind velocity that could trigger vortex shedding could range between 2 m/s and 40 m/s. Therefore, there could be the risk of observing vortices. However, ropes, nets, topmasts, yards, and several other components around the masts dramatically increase the vortex-shedding triggering wind velocity. Owing to its periodicity and transverse forcing nature, the expected gust responses are likely to retain spatially local character. The frequency of shed vortices depends on the steady airstream velocity; however, this factor varied during the acquisition period. Consequently, the locality, directionality and unsteadiness arguments are used to exclude this possible mechanism as the underlying cause behind the dominant frequency features observed in the stabilisation diagram.

While the stabilisation diagram alone, adopted in the OMA context, cannot provide conclusive evidence of the modal behaviour of the structural system, the subsequent analysis of the vibration patterns associated with the selected frequencies can be used to assess the expected global character of the identified modes.

Considering the above discussion and to further investigate the results, the spatial dynamic activity corresponding to the measured channels is studied. For that purpose, the response PSD matrix is constructed by combining the data from all measured channels. The analysis of the PSD matrix at the identified dominant frequencies is used to establish the vibration pattern experienced by the structure at that frequency (Brincker 2014). Under the general test conditions, these patterns correspond to the Operational Deflection Shapes (ODS). If the selected frequency is the natural frequency, the identified dynamic pattern tends to be strongly dominated by the corresponding mode shape. Another aspect of the identified ODS is their complex-valued character, which is indicative of the relative phase delays in response between different measurement locations at the specific frequency. Under ideal OMA conditions (Brincker 2014) and under the assumption of linear viscous damping, these phase delays can be further attributed to the non-proportional damping distribution in the measured system. The calculated ODS vectors can be mapped onto the actual measurement physical locations and, combined with judiciously adopted assumptions regarding the structural disposition and boundary conditions, used to visualise the corresponding dynamic activity. This OMA step permits the spatial contextualisation of the dynamic activity associated with the selected frequencies. Owing to its potential relationship with the support system, this visual insight can further highlight the significance of the corresponding motion patterns for further diagnostic and monitoring purposes.

Only a fraction of the signals (i.e. 3 minutes, corresponding to 90,000 samples) not dominated by high acceleration peaks was used for this analysis to minimise the risk of observing non-modal dynamics. Figure 11 shows the ODS corresponding to some of the selected candidate frequencies.

As per Figure 7, the triangular shape idealises the hull; the grey area represents the ship's weather deck. The black points in the figure show the locations of the sensors. The black dashed lines represent the undeformed structure; the blue lines represent the geometry of the vibrating system. The points at the base where there are no sensors are assumed to be fixed as these correspond to the keel beam points standing on timber blocks. Using the terminology defined in Figure 2, it can be observed that the 2.4 Hz case corresponds to a roll rotation, the 4.1 Hz ODS corresponds to a yaw rotation, and the 6.2 Hz corresponds to a pitch rotation. Also, the 7.9 Hz frequency corresponds to a predominantly vertical vibration of the hull. In Figure 11, each ODS is accompanied by its Argand diagram, showing the real and imaginary parts of the complex-valued ODS vectors. These diagrams clearly show the phase relationships between the individual measured channels as well as their oscillatory in and out-of-phase vibration characteristics. Further, the lack of close linear alignment between the individual ODS vector components can be attributed to the system damping and its spatial properties. In this way, this property might constitute a feature sensitive to system changes suitable for SHM purposes.

To support an argument that the above frequencies can be associated with the modal dynamics, a study is performed to show that they are located within the range of analytically obtained approximate predictions. Following the assumptions introduced in Figure 2, a simple ship rolling model is used in Appendix B. Considering the parameter uncertainties involved in this dynamic description of the system, the distribution of all possible roll frequencies obtained propagating the uncertainties is presented. The roll frequency histogram suggests that this natural frequency is indeed located in the region approximately centred around 3 Hz. Owing to the flexibility of the real system, the slightly lower frequency of 2.4 Hz is deemed to be correctly identified as being the actual rolling frequency the ship. The corresponding ODS visualisation suggests constant lengthwise sectional shearing, which can be interpreted as the ship's rolling response to dry dock conditions. The ODS, therefore, provides an interpretative context that can be used to explain the differences between the two sets of results.

These results confirm that relatively short dynamic response observation campaigns can provide sufficient information to carry out Operational Modal Analysis under the conditions of significant unsteady winds.

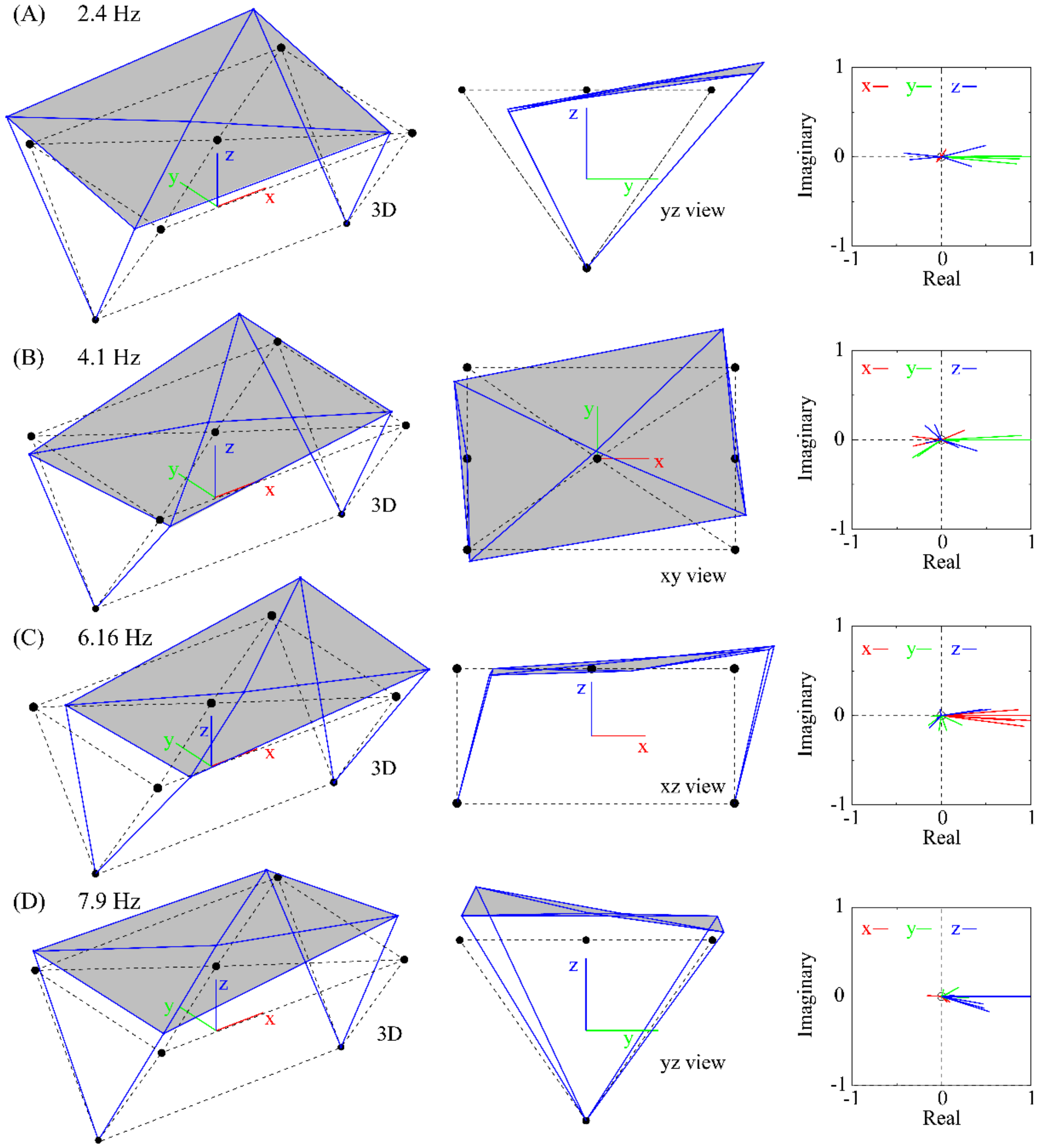

Figure 11 – Operational displacement shapes corresponding to (A) 2.4 Hz, (B) 4.1 Hz, (C) 6.16 Hz, and (D) 7.9 Hz. The points at the base where there are no sensors are assumed to be fixed as these correspond to the keel beam points standing on timber blocks.

5.2 Cutty Sark

For this case study, a 12-hour monitoring test was conducted. The test was mainly performed during the nighttime to avoid interaction with visitors for health and safety reasons. Although the data acquisition was longer compared to the SSGB, the lack of strong winds or other human-induced excitations directly on the ship makes interpreting this study more challenging. The acquired data were split into portions of 3-hour signals. In this paper, only the last three hours will be presented (roughly between 5:00 am and 8:00 am); however, the same conclusions can be drawn by looking at any portion of the acquired signals. Figure 12 shows the signals, in terms of accelerations, acquired by the sensor B5 during the last three hours of recording for the x, y, and z directions (Figure 6B). Similar results are obtained for all other sensors. The accelerations recorded along the vertical direction are slightly larger than those along the longitudinal and transverse directions. Also, the spectrogram for the three signals is provided. These spectrograms show that it is possible to visually discern the frequency features from the signal (see frequencies below 10 Hz) for the longitudinal and transverse directions. In terms of structure and features, the results in the vertical direction are less clear. Similarly to the previous case study, it is possible to conclude that the sensors provide usable data, even in lack of strong wind excitation (average wind velocities below 4m/s). Furthermore, as the frequency features do not visibly change with the observation time, it is concluded that no significant non-stationarity is observed.

It is worth noting that acceleration levels, notwithstanding the quietness during the monitoring period, are not too dissimilar from those for SSGB in Figure 8. However, in this case, a significant fraction of the signal's energy is concentrated in the frequency range above 12 Hz. As expected, this is confirmed by the fact that the pass-filtered signal for the range of frequencies between 0.2 Hz and 12 Hz (shown in grey colour in Figure 12) is lower with respect to the pass-filtered signal for the frequency range between 0.2 Hz and 50 Hz. Further, it can be seen that the instantaneous step changes in the signals' profile are absent in the signals filtered in the narrower frequency range of interest. These effects are, therefore associated with high-frequency non-environmental and possibly localised sources. Precisely, the sudden increase of the vertical acceleration levels after the first acquisition hour corresponds to the activation of a ventilation unit at around 6 am. Finally, the peaks that are visible at the end of the time series are induced by the human activity associated with the morning security checks on the deck and by our team's arrival to supervise the monitoring system.

Figure 13 shows the Power Spectral Density (PSD) plots for all the sensors for both accelerations and displacements (obtained by dividing the acceleration amplitude by the square of the circular frequency) for the three directions, x, y, and z, separately. Results show that almost all PSD plots overlay, indicating global modal activity of the supporting structural system in the frequency range of interest. Clear peaks can be identified for all three directions; moreover, some peaks are common for more than one direction, indicating the presence of spatially coupled modes. As expected from Figure 2, this spatial coupling can lead to the expected rotational modes or more complex vibration forms, such as those implying sectional shearing. The PSD of sensor B7 shows a significant difference compared to the others, especially for the z direction. This effect is identified with a local vibration of the ship's central mast. Similar behaviour was observed in the SSGB study for sensor A5, which is located close to one of the masts. Finally, the presence of a comparatively weak wind excitation in this case study can be clearly observed when contrasting the PSD response levels reported in Figure 13 with those recorded in Figure 9 for the SS Great Britain.

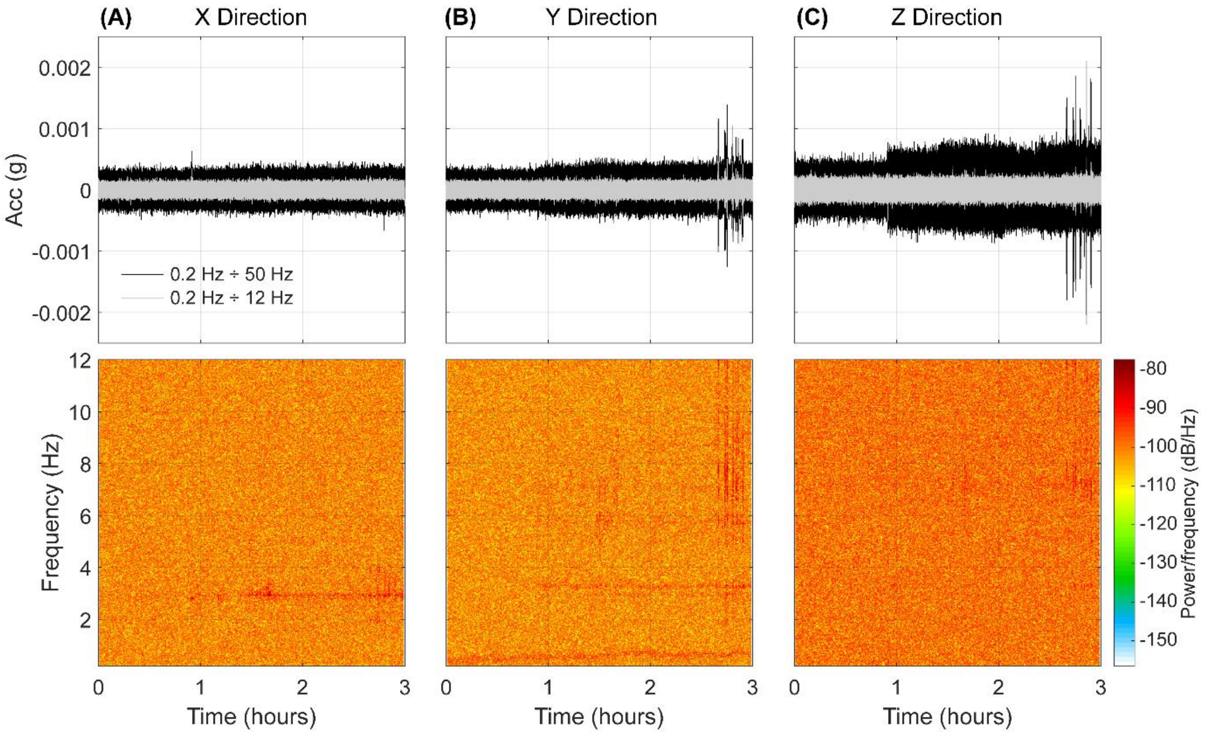

Figure 12 – Acceleration and spectrogram for the sensor B5 and for the (A) x, (B) y, and (C) z directions.

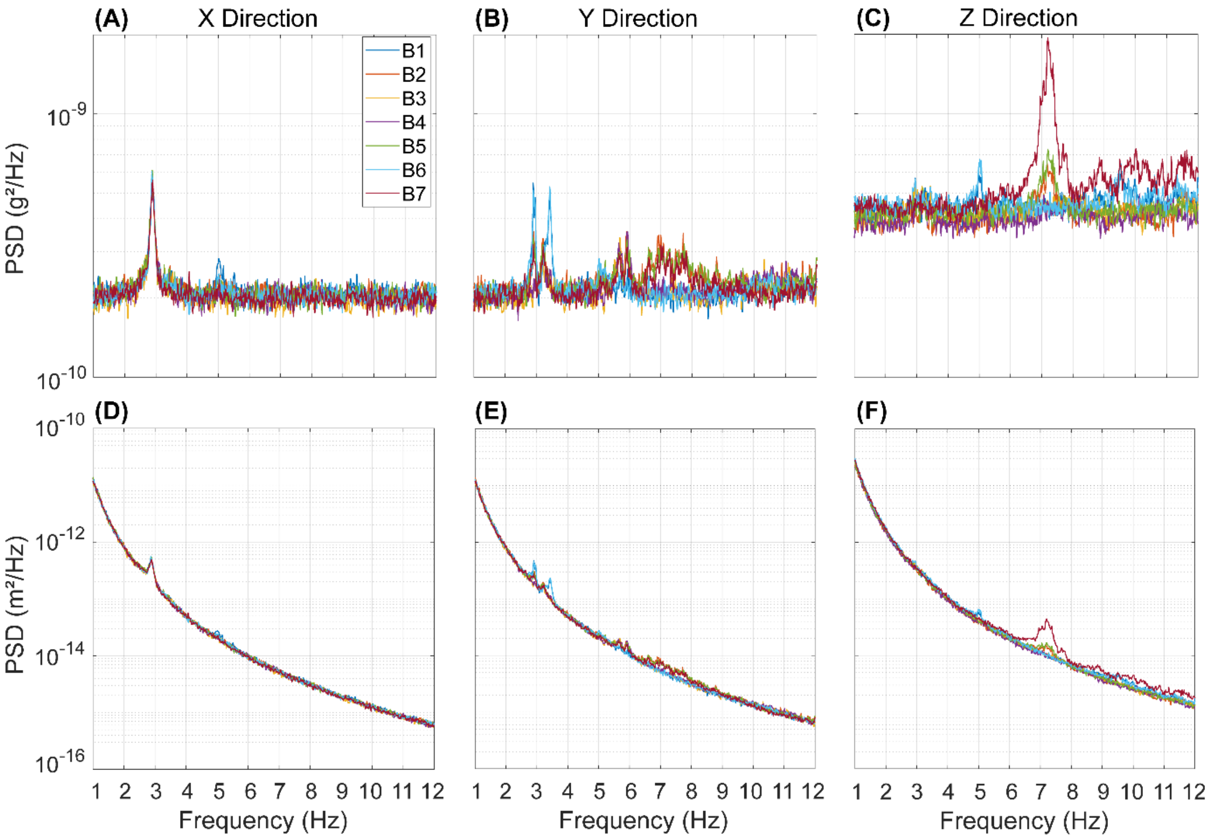

Figure 13 – Welch's Power Spectral Density plots for all sensors and for the (A,D) x, (B,E) y, and (C,F) z directions in terms of accelerations (A-C) and displacements (D-F).

As anticipated in Section 2.2, and as already done in Section 4.1, the stabilisation diagram is used to identify the observable natural frequencies located within the chosen frequency range. The corresponding ODSs are used to confirm that these frequencies are associated with global oscillatory activity characteristic of the low-frequency vibration modes. This analysis is reported in Figure 14. From the diagram, it emerges that, despite the low response levels, there are several clear frequencies found, and the damping associated with them ranges between 1.4% and 2.7%. The SVD approach (Brincker and Ventura, 2015) is used to extract the corresponding ODS. To avoid potential pollution of the data used here by the discrete and deterministic sources of excitation, a 15-minute-long (i.e. 450,000 samples) part of the last 3-hour signals, free from high impulsive acceleration peaks, was used for this analysis.

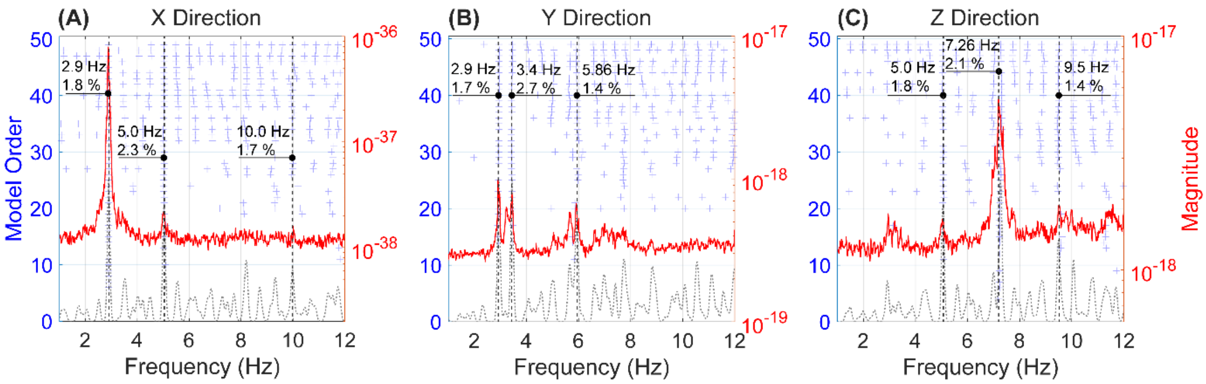

Figure 14 – Stabilisation diagram for all sensors and for the (A) x, (B) y, and (C) z directions.

Figure 15 shows the selected ODS corresponding to the candidate frequencies. As before, the triangular shape idealises the hull's cross-section; the grey area represents the ship's deck.

The black points in the figure represent the locations of the sensors. As the ship is suspended and the keel beam is not connected to the ground, the points at the base of the triangular shape are assumed to have a displacement equal to the average of the two points on the same cross-section on the weather deck. Using the terminology defined in Figure 2, it can be observed that the 2.9 Hz vibration pattern corresponds to a longitudinal translation, the 3.4 Hz corresponds to the yaw rotation, the 5.0 Hz corresponds to a longitudinal mode with a flexural component of the ship (where a similar pattern can be observed again for the 9.5 Hz frequency); finally, the 7.9 Hz corresponds to a vertical vibration mode with a great intensification of the central mast vertical displacement. From this section, it is possible to conclude that, for historic ships in dry docs, short-term monitoring can yield results suitable for carrying out a complete Operational Modal Analysis even when significant wind effects or human-induced vibrations are absent.

It is interesting to note the difference between the fundamental ODS identified in the two studies. While the SSGB, with its grounded keel beam, features the first rolling vibration pattern combined with sectional shearing, the suspended Cutty Sark's first major vibration pattern is dominated by the longitudinal translation. Hence, in both cases, the nature of the support system strongly influences the characteristics of the fundamental mode, which, in turn, plays a significant role in forced dynamic responses caused by ground motions or wind effects. This is where the OMA results can find their first direct application. For instance, the identified damping ratio is around 2 % in both cases. This is a relatively low value traceable to the structural and material composition of the support system, which can cause significant amplification of dynamic responses compared to their equivalent static counterparts. In the case of a single-degree-of-freedom approximation of the problem at hand, such a damping value would result in a dynamic amplification of around 25.

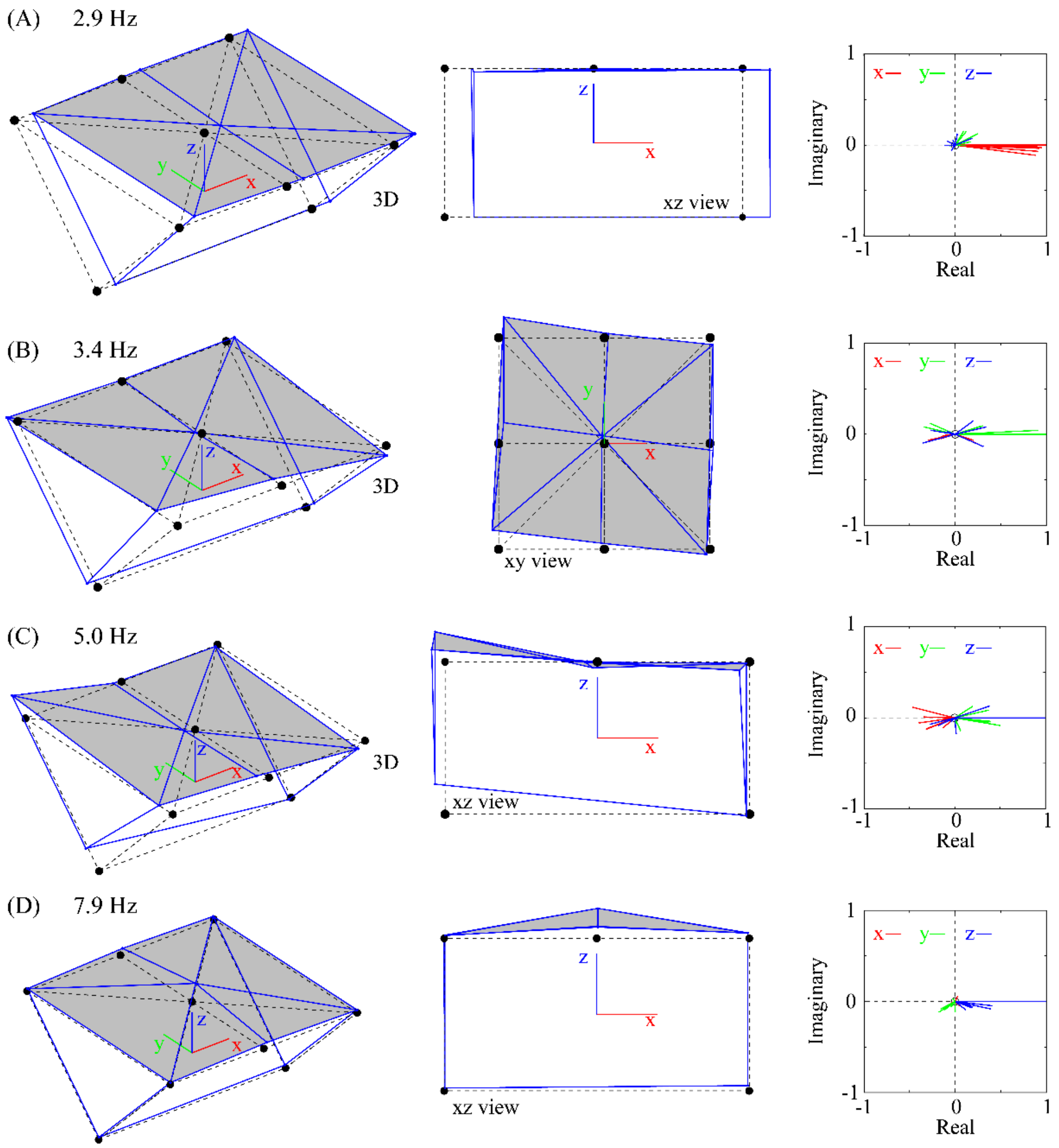

Figure 15 – Operational displacement shapes corresponding to (A) 2.9 Hz, (B) 3.4 Hz, (C) 5.0 Hz, and (D) 7.9 Hz. The points at the base where there are no sensors are assumed to be moving together with the two points on the same cross-section on the weather deck.

The results presented in the two case studies show that the OMA approach can be used to determine the inherent vibration characteristics of the ships and that these are strongly influenced (as demonstrated by the identified ODS and natural frequencies) by the specifics of the dry-docking support system. When considering the SHM application of this methodology, owing to their global nature, robust identification potential and close links with the properties of the support system, various attributes of the identified fundamental vibration modes can serve as damage-sensitive features. For instance, the combined use of the natural frequency and symmetry assessment of the corresponding ODS could be used to monitor the potential loss or deterioration of the individual support members. Alternatively, the value of the modal damping might be more sensitive to the emergence of new significant energy dissipation sources that are traditionally associated with the loss of structural fasteners or the creation of new friction or crack interfaces.

5. Conclusions

Historic ships permanently sitting in dry docks are a key component of worldwide nations' maritime cultural heritage. However, their delicate nature and the features of dry docks and structural support systems make the conservation of such assets very challenging.

This paper demonstrated that vibration-based SHM can be further developed using the established OMA methods as a non-destructive "sympathetic" method to gain data about the current status of the ship-support-dock system. The research results demonstrated that conventional accelerometers can be used to conduct a complete and comprehensive Operational Modal Analysis of dry-docked historic ships.

Two case studies were investigated: (1) the SS Great Britain in Bristol and (2) the Cutty Sark in London. Although these two case studies had several differences (e.g., ship material, support system, number of sensors and the wind velocity during monitoring), the post-processing of the acquired data establishes shared insights on the used approach:

- Significant insights regarding the modal mobility can be obtained by means of a preliminary Operational Modal Analysis based on short-term time series recorded on the weather deck of historic ships in dry docks;
- The presence of wind does not reduce the significance of the dynamic outputs even if the interaction with the masts can be non-trivial;
- Due to early emergence of flexible vibration modes in the low frequency range, at least four multi-axial sensors should be used to monitor dry-docked ships in order to distinguish basic operational deflection shape patterns associated with possible ship's hull and deck twisting, shearing and warping.
- The main natural frequencies lay in the range between 1 and 10 Hz for both conventional (struts and blocks) and non-conventional (suspended) supporting systems.

Therefore, this paper demonstrated the possibility of using vibration-based SHM to obtain information on the current state of historical maritime assets for their preventive conservation. It further informs the practical requirements for future efforts that will aim to reach similar or better SHM resolution. Although specific preventive actions were not mentioned in this research, the information obtained represent a diagnostic tool as it can constitute the baseline reference for future investigations and can guide future conservation efforts. For instance, changes in these vibration characteristics can indicate deterioration or damage, prompting further investigation and maintenance.

Future research should focus on using damage-detection algorithms (such as the High-Order Spectral Analysis) based on the principles proved in this paper. Moreover, this study focused on wind effects mainly; there is a need for comprehensive environmental monitoring in future efforts. Potential research should also aim to incorporate geotechnical aspects more thoroughly.

Acknowledgements

We thank the SS Great Britain Trust and the Royal Museums Greenwich for allowing us to monitor the two ships. Raffaele De Risi acknowledges the project CIRCLE (ES/Z000122/1).

Also, when we monitored the Cutty Sark, Maria Bastidas-Spence was employed at Royal Museums Greenwich as a Preventive Conservator, overseeing collection care strategies for various sites, including the Cutty Sark.

Appendix A

Before the application in the field, the sensors have been tested on the shaking table available in the EQUALS laboratory at the University of Bristol. Three sensors have been tested together (Figure A1-A); one sensor was fixed to the table using a magnetic stand (Figure A1-B), one sensor was connected using hot glue (Figure A1-C), and one sensor was connected rigidly to the table surface using steel clamps (Figure A1-D).

The sensors connected with hot glue and with the magnetic stand needed some additional layers for the connection to the shaking table. Specifically, for the hot glue connection (Figure A1-E), the sensor is screwed to a Perspex plate that is then glued to the table surface. For the magnetic stand, the sensor is screwed on a tick timber plate in which some magnets are installed in specific drilled recesses (Figure A1-F). The sensor is then simply located on a steel plate that is clamped on the table (as the table surface is made of aluminium, and, therefore, it is diamagnetic).

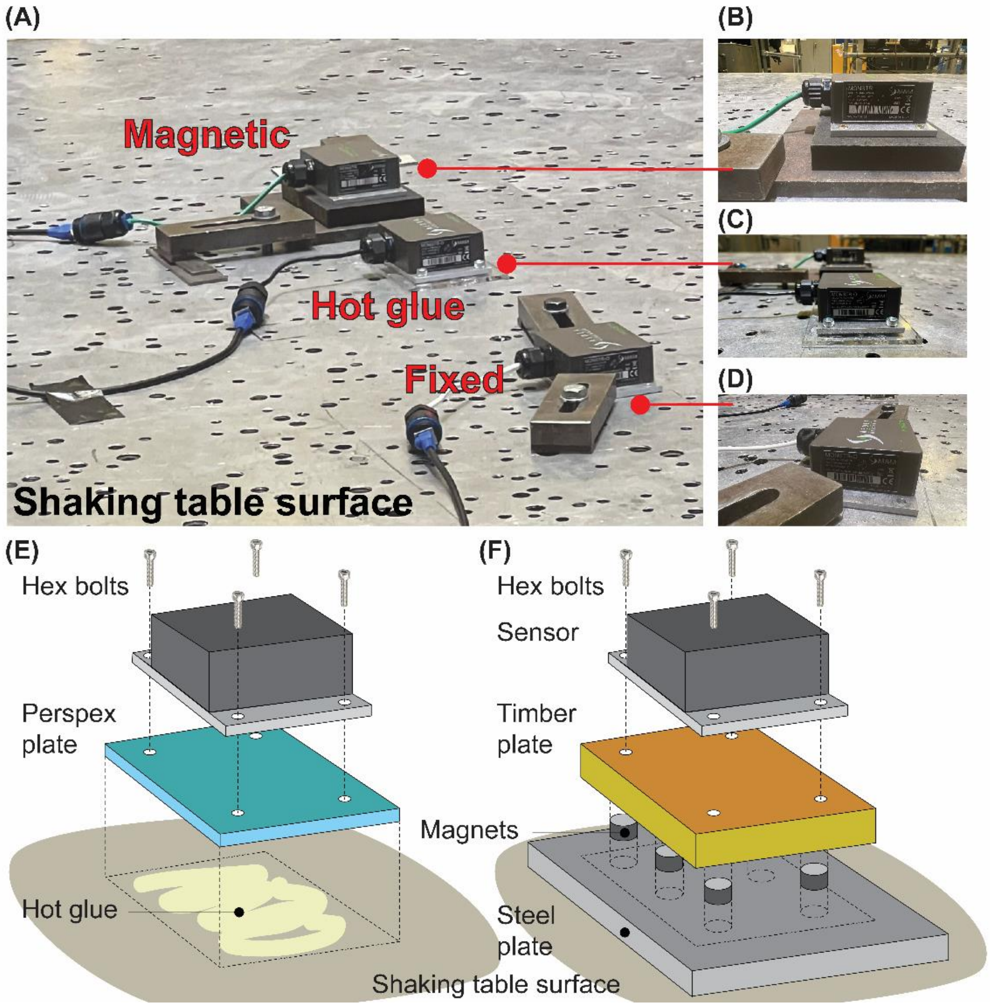

Figure A1 – (A) Sensors on the shaking table; (B) magnetic stand, (C) hot-glue connection, and (D) fixed to the table. Schematic representation of the (E) hot-glue connection and (F) magnetic connection.

Several white noises at increasing amplitude have been applied to the three sensors in all three directions. As an example, Figure A2 shows the PSD in terms of accelerations and displacements for the three different connections for the y-direction and for white noise with a maximum acceleration of 1.5g. It is possible to observe that the three PSDs are perfectly overlapping. Also, the glued and magnetic connections have a coherency equal to 1 (Figure A2-C) with respect to the sensor rigidly clamped to the table.

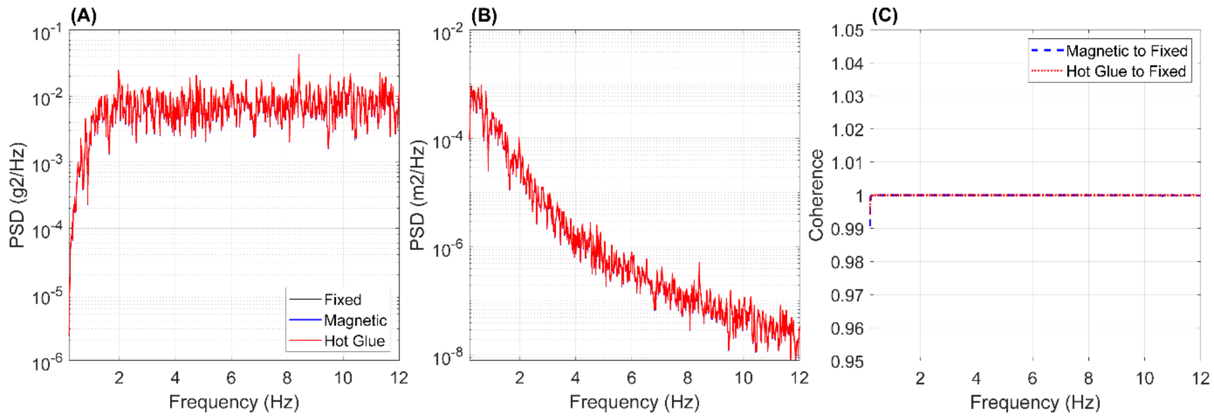

Figure A2 Welch's Power Spectral Density plots for the three connections in terms of accelerations (A-C) and displacements (D-F).

Judging by the results and considering the small mass of the sensors (i.e. the small inertia), it is possible to conclude that sensors can be safely used with the proposed connections up to 1.5g; however, we suggest not to exceed 1.0g as a safety precaution.

Appendix B

This appendix shows the crude dynamic model of a ship on supports based on the schematisation presented in Figure 2. The focus is the roll frequency. However, similar discussion can be done for the pitch and the yaw.

Let us consider the following figure. The vertical struts can be idealised as springs with vertical stiffness $K_Z = EA/L_Z$, where E is steel Young's Modulus, A is the area of the cross section of the struts, and L_Z is the height of the struts. The horizontal distance between the struts is L_Y. Finally, m is the mass of the ship.

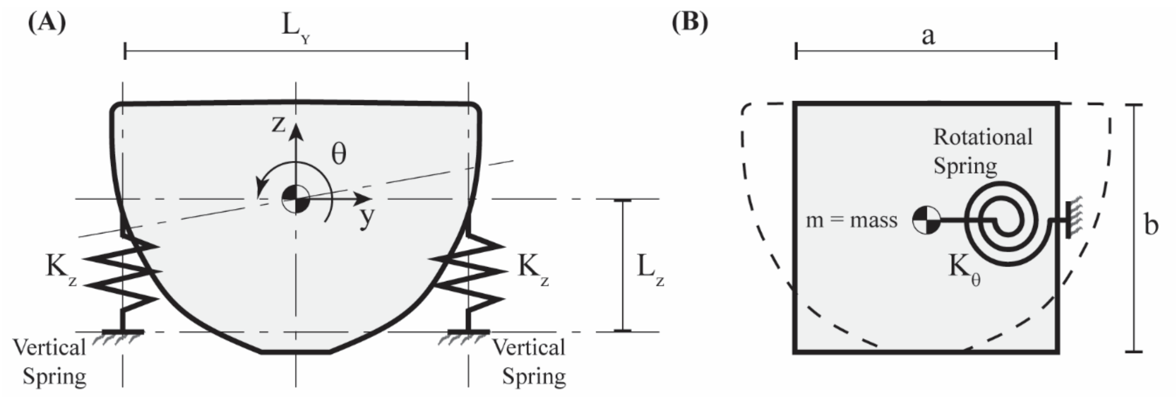

Figure B1 – (A) Actual configuration and (B) simplified scheme for the roll behaviour.

If not available, the actual cross-section of the ship Figure B1(A) can be simplified with a rectangular shape with approximated width a and height b. Moreover, the two vertical struts can be considered as working in compression-only; therefore, the rotational stiffness can be computed imposing a rotation θ equal to 1 as:

$$K_\theta = K_Z \frac{L_Y^2}{4} \quad \text{B1}$$

The polar mass moment of inertia is given by:

$$M_\theta = m \frac{I_Y + I_Z}{a \cdot b} \quad \text{B2}$$

Where IY and IZ are the moment of inertia of the rectangle around the vertical and horizontal axis:

$$I_Y = \frac{a \cdot b^3}{12} \qquad I_Z = \frac{a^3 \cdot b}{12} \quad \text{B3}$$

and $a \cdot b$ is the area of the cross-section.

The frequency of the system associated with the roll can be then computed as:

$$f = \frac{1}{2\pi} \sqrt{\frac{K_\theta}{M_\theta}} \quad \text{B4}$$

Not all the variables presented in this model could be necessarily available. Therefore, the following assumptions are made: a=13m, b=10m; the mass is assumed to span between 1500 and 4000 tons, E=207GPa, the external diameter of the supports = 114.3mm (this is known); the thickness of walls of the struts varying between 4 and 6 mm; the number of prop lines = 13; L_Z spanning between 3 and 5m; L_Y spanning between 7 and 12 m. Assuming a uniform distribution of all the parameters, more than 4000 combinations of parameters are obtained, and the frequencies presented in Figure B2 are computed. The median roll frequency is around 3 Hz, which is very close to the identified roll frequency of 2.4 Hz. Most interestingly, the range of computed frequencies is between 1 Hz and 10 Hz, which is the range of the observed frequencies as well.

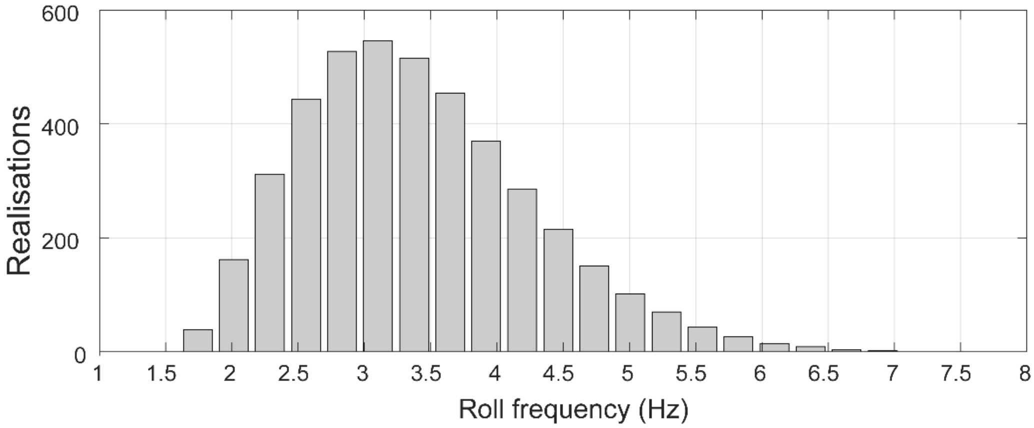

Figure B2 – Realisations of possible roll frequencies obtained propagating the uncertainties presented above.

This analysis can be replicated for the yaw and the pitch rotations using the Courbon (1976) approximation. For these cases, the obtained frequencies span between 4 and 10 Hz with a median of about 5.5Hz for the yaw and 6Hz for the pitch. The simplified models and the results are not provided entirely for brevity.

References

Aberg, A. (2005). Saving the victory. *The Mariner's Mirror*, 91(2), 358-368. https://doi.org/10.1080/00253359.2005.10656955.

Abu Shehab, H., Kishida, T., Bouchaala, F., Patel, S., Voyagaki, E., Kim, T. Y., & Al Shehhi, M. R. (2024). Strategic Placement of Accelerometers for Structural Health Monitoring of a Complex Unreinforced Stone Masonry Hindu Mandir. *International Journal of Architectural Heritage*, 1-19. https://doi.org/10.1080/15583058.2024.2323031.

Aceto, L., Amelio, A., Boccagna, R., Bottini, M., Camata, G., Germano, N., & Petracca, M. (2022, August). A Self-Consistent Artificial Intelligence-Based Strategy for Structural Health Monitoring. In Fifth International Conference on Railway Technology: Research, Development and Maintenance (RAILWAYS 2022).

Akan, A., & Chaparro, L. F. (2024). Signals and systems using MATLAB®. Elsevier.

Alaggio, R., Aloisio, A., Antonacci, E., & Cirella, R. (2021). Two-years static and dynamic monitoring of the Santa Maria di Collemaggio basilica. *Construction and Building Materials*, 268, 121069. https://doi.org/10.1016/j.conbuildmat.2020.121069.

Ardakani, V. G., Gambaruto, A. M., Grahamslaw, N., Garsed-Brand, G., Ault, R., Vaquero, E., & Pregnolato, M. (2023). Heritage conservation with a surface air curtain: Use of CFD and sensor data with a near-wall region flow analysis. *Building and Environment*, 243, 110640. https://doi.org/10.1016/j.buildenv.2023.110640.

Azzara, R. M., Girardi, M., Iafolla, V., Lucchesi, D. M., Padovani, C., & Pellegrini, D. (2021). Ambient vibrations of age-old masonry towers: Results of long-term dynamic monitoring in the historic centre of Lucca. *International Journal of Architectural Heritage*, 15(1), 5-21. https://doi.org/10.1080/15583058.2019.1695155.

Barsocchi, P., Bartoli, G., Betti, M., Girardi, M., Mammolito, S., Pellegrini, D., & Zini, G. (2021). Wireless sensor networks for continuous structural health monitoring of historic masonry towers. *International Journal of Architectural Heritage*, 15(1), 22-44. https://doi.org/10.1080/15583058.2020.1719229.

Boccagna, R., Bottini, M., Petracca, M., Rossi, M., Amelio, A., & Camata, G. (2023). Integrating Data-driven and Model-based Algorithms for Structural Health Monitoring. In *14th International Conference on Application of Statistics and Probability in Civil Engineering*.

Bongiovanni, G., Buffarini, G., Clemente, P., & Saitta, F. (2021). Time and frequency domain analyses in the experimental dynamic behaviour of the Marcus Aurelius' column. *International Journal of Architectural Heritage*, 15(1), 64-78. https://doi.org/10.1080/15583058.2019.1706785.

Brincker, R. (2014). Some elements of operational modal analysis. *Shock and Vibration*, 2014(1), 325839. http://dx.doi.org/10.1155/2014/325839.

Brincker, R., & Ventura, C. (2015). Introduction to operational modal analysis. John Wiley & Sons.

Ceravolo, R., Pistone, G., Fragonara, L. Z., Massetto, S., & Abbiati, G. (2016). Vibration-based monitoring and diagnosis of cultural heritage: a methodological discussion in three examples. *International Journal of Architectural Heritage*, 10(4), 375-395. https://doi.org/10.1080/15583058.2013.850554.

Cigada, A., Corradi Dell'Acqua, L., Mörlin Visconti Castiglione, B., Scaccabarozzi, M., Vanali, M., & Zappa, E. (2017). Structural health monitoring of an historical building: the main spire of the Duomo Di Milano. *International Journal of Architectural Heritage*, 11(4), 501-518. https://doi.org/10.1080/15583058.2016.1263691.

Civera, M., Pecorelli, M. L., Ceravolo, R., Surace, C., & Zanotti Fragonara, L. (2021). A multi-objective genetic algorithm strategy for robust optimal sensor placement. *Computer-Aided Civil and Infrastructure Engineering*, 36(9), 1185-1202. https://doi.org/10.1111/mice.12646.

Clementi, F., Formisano, A., Milani, G., & Ubertini, F. (2021). Structural health monitoring of architectural heritage: From the past to the future advances. *International Journal of Architectural Heritage*, 15(1), 1-4. https://doi.org/10.1080/15583058.2021.1879499.

Courbon, J. (1976). Design of multi-beam bridges with intermediate diaphragms: Calculation of multiple beam bridges solidarized by spacers. *Annals of Bridges*, 1976, 115-116.

Davenport, A. G. (1961). The spectrum of horizontal gustiness near the ground in high winds. *Quarterly Journal of the Royal Meteorological Society*, 87(372), 194-211. https://doi.org/10.1002/qj.49708737208.

Davis, C. (2024). Restricted Access to Remembrance: Problematic Usages of Industrial Memories in Belfast's Titanic Quarter. *Studies in Ethnicity and Nationalism*, 24(1), 55-70. https://doi.org/10.1111/sena.12412.

Dumont, M., Cook, A., & Kinsley, N. (2016). Acceleration measurement optimization: mounting considerations and sensor mass effect. In Topics in Modal Analysis & Testing, Volume 10: Proceedings of the 34th IMAC, A Conference and Exposition on Structural Dynamics 2016 (pp. 61-71). Springer International Publishing.

Douglas, L. (2012). The Cutty Sark is back. *Engineering & Technology*, 7(9), 68-71. https://doi.org/10.1049/et.2012.0908.

Fiorentino, G., Quaranta, G., Mylonakis, G., Lavorato, D., Pagliaroli, A., Carlucci, G., ... & Nuti, C. (2019). Seismic reassessment of the leaning tower of Pisa: Dynamic monitoring, site response, and SSI. *Earthquake Spectra*, 35(2), 703-736. https://doi.org/10.1193/021518EQS037M.

Formisano, A., Di Lorenzo, G., Krstevska, L., & Landolfo, R. (2021). Fem model calibration of experimental environmental vibration tests on two churches hit by L'Aquila earthquake. *International Journal of Architectural Heritage*, 15(1), 113-131. https://doi.org/10.1080/15583058.2020.1719233.

Gonzalez-Fernandez, D., De Risi, R., Rezgui, D., Macdonald, J. H., Margnelli, A., & Titurus, B. (2023, October). Identification of varying modal parameters of a tall building from the full-scale wind-induced responses. *Structures*, 56, 104770. https://doi.org/10.1016/j.istruc.2023.06.101.

Guillaume, P. (2006). Multivariable frequency-domain system identification algorithms for modal analysis. *IFAC Proceedings Volumes*, 39(1), 94-109. https://doi.org/10.3182/20060329-3-AU-2901.00008.

Hageman, R. B., & Drummen, I. (2019). Modal analysis for the global flexural response of ships. *Marine Structures*, 63, 318-332. https://doi.org/10.1016/j.marstruc.2018.09.012.

House, D. (2015). Dry docking and shipboard maintenance: A guide for industry. Routledge.

Jayatilake, S. D., Lowenberg, M., Woods, B. K. S., & Titurus, B. (2024). Systematic Experimental Evaluation of Aeroelastic Characteristics of a Highly Flexible Wing Demonstrator. *AIAA Journal*, 62, 4615-4630. https://doi.org/10.2514/1.J064058.

Kammer, D. C. (1991). Sensor placement for on-orbit modal identification and correlation of large space structures. *Journal of Guidance, Control, and Dynamics*, 14(2), 251-259. https://doi.org/10.2514/3.20635.

Karanikoloudis, G., Lourenco, P. B., Mendes, N., Serra, J. B., & Boroschek, R. (2021). Monitoring of induced groundborne vibrations in cultural heritage buildings: miscellaneous errors and aliasing through integration and filtering. *International Journal of Architectural Heritage*, 15(1), 205-228. https://doi.org/10.1080/15583058.2020.1802532.

Lin, B., & Dong, X. (2023). Ship hull inspection: A survey. *Ocean Engineering*, 289, 116281. https://doi.org/10.1016/j.oceaneng.2023.116281.

MATLAB, 2023. Version: 9.14.0.2206163 (R2023a), Natick, Massachusetts: The MathWorks Inc.

Milani, G., & Clementi, F. (2021). Advanced seismic assessment of four masonry bell towers in Italy after operational modal analysis (OMA) identification. *International Journal of Architectural Heritage*, 15(1), 157-186. https://doi.org/10.1080/15583058.2019.1697768.

Millar, O., Thomas M., and Monasta, J. (2024). Historic ships and docks: a marriage of convenience or the perfect union? Available at: https://beckettrankine.com/wp-content/uploads/2024/09/icmm-congress-24_historic-ships-and-docks-paper.pdf. Accessed 01/12/2024.

Mitra, S. K. (2001). Digital signal processing: a computer-based approach. McGraw-Hill Higher Education.

Nikias, C. L., & Mendel, J. M. (1993). Signal processing with higher-order spectra. *IEEE Signal processing magazine*, 10(3), 10-37. https://ieeexplore.ieee.org/document/221324.

Oppenheim A.V., Schafer R.W. (1989). Discrete-time signal processing. Prentice-Hall.

Otter, R.A. (2003). The construction of dry docks: Some nineteenth-century perspectives. *Transactions of the Newcomen Society*, 73(2), 241-255. https://doi.org/10.1179/tns.2003.012.

Pecorelli, M.L., Ceravolo, R., & Epicoco, R. (2020). An automatic modal identification procedure for the permanent dynamic monitoring of the Sanctuary of Vicoforte. *International Journal of Architectural Heritage*, 14(4), 630–644. https://doi.org/10.1080/15583058.2018.1554725.

Peeters, B., Van der Auweraer, H., Guillaume, P., & Leuridan, J. (2004). The PolyMAX frequency-domain method: a new standard for modal parameter estimation?. *Shock and Vibration*, 11(3-4), 395-409. https://doi.org/10.1155/2004/523692.

Pregnolato, M., Gunner, S., Voyagaki, E., De Risi, R., Carhart, N., Gavriel, G., ... & Taylor, C. (2022). Towards Civil Engineering 4.0: Concept, workflow and application of Digital Twins for existing infrastructure. *Automation in Construction*, 141, 104421. https://doi.org/10.1016/j.autcon.2022.104421.

Rainieri, C., & Fabbrocino, G. (2014). Operational modal analysis of civil engineering structures. Springer, New York, 142, 143.

Rehler, J., & Bottger, G. (1964). Dry docks through five centuries. *The Military Engineer*, 56(369), 43-45. https://www.jstor.org/stable/44574340.

Rosso, M. M., Aloisio, A., Parol, J., Marano, G. C., & Quaranta, G. (2023). Intelligent automatic operational modal analysis. *Mechanical Systems and Signal Processing*, 201, 110669. https://doi.org/10.1016/j.ymssp.2023.110669.

Schleihauf, W. (2000). The Restoration of HMS M-33. *Warship International*, 37(2), 170-176.

Standoli, G., Giordano, E., Milani, G., & Clementi, F. (2021). Model updating of historical belfries based on oma identification techniques. *International Journal of Architectural Heritage*, 15(1), 132-156. https://doi.org/10.1080/15583058.2020.1723735.

Vickery, B. J., & Basu, R. I. (1983). Across-wind vibrations of structures of circular cross-section. Part I. Development of a mathematical model for two-dimensional conditions. *Journal of Wind Engineering and Industrial Aerodynamics*, 12(1), 49-73. https://doi.org/10.1016/0167-6105(83)90080-6.

Waite, S. T. (1997). The Pros & Cons of Permanently Dry-Docking Historic Vessels. In Proceedings of the Third International Conference on the Technical Aspects of the Preservation of Historic Vessels, San Francisco 20-23 April 1997.

Watkinson, D., Tanner, M., Turner, R., & Lewis, M. (2005). ss Great Britain: teamwork as a platform for innovative conservation. *The conservator*, 29(1), 73-86. https://doi.org/10.1080/01410096.2005.9995214.